The thermal stabilities of these compounds are dependent on the extent of ligand methylation, while structural dissimilarities are due to the steric requirements dictated by the particular substitution pattern. Work is proceeding to further examine the effect of methylation on thermal stability and to investigate the potential of these Cp*–allyl dihalide compounds as starting points for the synthesis of other Cp*–allyl complexes via halide substitution.

Acknowledgment is made to the donors of the Petroleum Research Fund, administered by the American Chemical Society, for the partial support of this research. This work was also supported, in part, through a Cottrell College Science Grant of Research Corp.

Registry No. 1, 109929-22-8; 2, 109929-23-9; 3, 109929-24-0; 4, 109929-25-1; 5, 109959-72-0; 6, 109959-71-9; Cp^*ZrCl_3, 75181-07-6.

Supplementary Material Available: Tables of thermal parameters and hydrogen atom coordinates (3 pages); listings observed and calculated structure factors (10 pages). Ordering information is given on any current masthead page.

Electrochemical, Structural, and Spectroelectrochemical Investigations of (OEP)Ir(CO)Cl and (TPP)Ir(CO)Cl in Nonbonding Media

C. Swistak, J.-L. Cornillon, J. E. Anderson, and K. M. Kadish*

Department of Chemistry, University of Houston, Houston, Texas 77004

Received February 27, 1987

The electrochemical and spectroelectrochemical properties of (P)Ir(CO)Cl, where P is the dianion of octaethylporphyrin (OEP) or tetraphenylporphyrin (TPP), are reported. These compounds can be reversibly oxidized by up to two one-electron transfer steps that occur at the porphyrin macrocycle. A two-electron reduction of (OEP)Ir(CO)Cl with ultimate formation of $[(OEP)Ir]^-$ is observed at room temperature. Low-temperature studies indicate that this reduction initially occurs at the porphyrin π ring system and that the anion radical intermediate can be stabilized. A self-consistent oxidation and reduction mechanism is presented. The molecular structure of (OEP)Ir(CO)Cl was found to crystallize in the $P2_1/c$ space group with a = 8.52 Å, b = 13.09 Å, c = 20.04 Å, β = 92.40°, and Z = 2.0.

Introduction

Synthesis of the iridium porphyrin (P)Ir(CO)Cl where P = a porphyrin dianion was first reported in 1968,[1] but it was not until 10 years later that the chemical reactivity of this compound was characterized in any detail.[2] (OEP)Ir(CO)Cl[3] can be converted to $(OEP)Ir(CH_3)$ by reaction with CH_3Li in THF. It may also be converted to (OEP)IrH and $[(OEP)Ir]^-$ by reduction with $NaBH_4$ in alkaline ethanol.[2] The hydride is the initial product in the synthesis of dimeric $[(P)Ir]_2$[4] while $[(P)Ir]^-$ can be converted to (P)Ir(R) by reaction with RX.[2]

Both dimeric $[(P)Ir]_2$ and the related σ-bonded (P)Ir(R) complexes have been the object of recent investigations.[4-6] It is known that (OEP)Ir(CO)Cl can be chemically reduced to give $[(OEP)Ir]^-$,[2,7] but a detailed electrochemical study of this reduction has never been presented. A structural characterization of (OEP)Ir(CO)Cl is also lacking in the literature.

(OEP)Ir(CO)Cl can be obtained as a product of the reaction involving $(OEP)H_2$ and either $[Ir(CO)Cl]_2$ or $[Ir(COD)Cl]_2$ where COD = 1,5-cyclooctadiene (eq 1).[2] In

$$(OEP)H_2 + [Ir(COD)Cl]_2 \rightarrow (OEP)Ir(C_8H_{13}) + (OEP)Ir(CO)Cl \quad (1)$$

a recent publication we presented the structural and electrochemical properties of $(OEP)Ir(C_8H_{13})$.[8] This paper presents the structural and electrochemical properties of (OEP)Ir(CO)Cl and the related (TPP)Ir(CO)Cl. The structure of (OEP)Ir(CO)Cl is only the second iridium porphyrin structure that has ever been obtained.

Experimental Section

Materials. Dichloromethane was purified by double distillation from CaH_2. Tetrahydrofuran (THF) (HPLC grade) was purified by distillation from Na/benzophenone. Benzonitrile (PhCN) (reagent grade) was vacuum distilled over P_2O_5. Tetrabutylammonium perchlorate ($TBAClO_4$) and tetrabutylammonium chloride (TBACl) were recrystallized twice from absolute ethanol, dried, and stored under vacuum at 45 °C. High-purity nitrogen and carbon monoxide were purchased from IWECO and Matheson, respectively. (OEP)Ir(CO)Cl and (TPP)Ir(CO)Cl were synthesized according to literature procedures.[1,2] The purity of these compounds was checked by comparison with reported ^1H NMR, UV–visible and IR spectra.

Instrumentation. Cyclic voltammetric measurements were performed with an EG&G Model 173 potentiostat, an EG&G Model 175 Universal programmer, and a Houston Instruments Model 2000 X-Y recorder or a BAS 100 electrochemical analyzer. Controlled potential electrolysis was performed with an EG&G Model 173 potentiostat or a BAS 100 electrochemistry system. Rotating disk electrode (RDE) experiments were performed with an IBM EC 1219 rotating disk electrode controller coupled with one of the above listed electrochemical instruments. Thin-layer spectroelectrochemical measurements were performed with an IBM EC 225 voltammetric analyzer which was coupled with a Tracor Northern 1710 holographic optical spectrometer multichannel analyzer to obtain spectral data either as a function of

(1) Sadasivon, N.; Fleischer, E. B. *J. Inorg. Nucl. Chem.* **1968**, *30*, 591.
(2) Ogoshi, H.; Setsune, J.; Yoshida, Z. *J. Organomet. Chem.* **1978**, *159*, 317.
(3) Abbreviations: OEP = 2,3,7,8,12,13,17,18-octaethylporphyrin dianion; TPP = 5,10,15,20-tetraphenylporphyrin dianion.
(4) Farnos, M. D.; Woods, B. A.; Wayland, B. B. *J. Am. Chem. Soc.* **1986**, *108*, 3659.
(5) Del Rossi, K. J.; Wayland, B. B., personal communication.
(6) Collman, J. P.; Kim, K. *J. Am. Chem. Soc.* **1986**, *108*, 7847.
(7) Sugimoto, H.; Ueda, N.; Mori, M. *J. Chem. Soc., Dalton Trans.* **1982**, 1611.
(8) Cornillon, J.-L.; Anderson, J. E.; Swistak, C.; Kadish, K. M. *J. Am. Chem. Soc.* **1986**, *108*, 7633.

0276-7333/87/2306-2146$01.50/0

Table I. Data Collection and Processing Parameters

mol formula	$IrClON_4C_{37}H_{44}\cdot 2C_7H_5N$
space group	$P2_1/c$, monoclinic
cell const	
a, Å	8.522 (3)
b, Å	13.086 (3)
c, Å	20.040 (4)
β, deg	92.40 (2)
V, Å^3	2233
fw	994.74
formula units per cell (Z)	2
density (ρ), g cm^{-3}	1.48
abs coeff (μ), cm^{-1}	30.81
radiatn (Mo Kα) (λ, Å)	0.710 73
collectn range, deg	$4 \le 2\theta \le 45$
scan width ($\Delta\theta$), deg	$0.90 + 0.35 \tan\theta$
max scan time, s	120
scan speed range, deg min^{-1}	0.7–5.0
total data collected	3291
independent data, $I > 3\sigma(I)$	2392
total variables	272
$R = \sum\|\|F_o\| - \|F_c\|\|/\sum\|F_o\|$	0.023
$R_w = [\sum w(\|F_o\| - \|F_c\|)^2/\sum w\|F_o\|^2]^{1/2}$	0.025

potential or as a function of time. The construction and properties of the optically transparent thin-layer electrode have been described in the literature.[9]

A conventional three-electrode system was used for all electrochemical experiments. The working electrode was a gold button of area 0.85 mm^2. The reference electrode was typically a commercial saturated calomel electrode, but in some cases a silver wire pseudoreference electrode was used. In both cases the reference electrode was separated from the bulk of the solution by a fritted glass bridge which contained the nonaqueous solvent and the supporting electrolyte. Potentials were referenced to the ferrocene/ferrocenium (Fc/Fc^+) couple when the silver wire pseudoreference electrode was used.

During controlled potential electrolysis the reference electrode and the platinum grid counter electrode were separated from the bulk solution by means of a fritted glass bridge. Unless otherwise noted, 0.1 M supporting electrolyte was used for electrochemical experiments. The porphyrin concentration ranged between 0.5×10^{-4} and 1×10^{-3} M.

An IBM Model ER 100D electron spin resonance system was used to record ESR spectra. IR spectra were taken on a IBM Model 32 FTIR spectrophotometer.

Crystal Structure Determination. Single-crystal X-ray analysis of (OEP)Ir(CO)Cl was performed at the University of Houston X-Ray Crystallography Center. A $0.70 \times 0.35 \times 0.30$ mm section of a very long, dark magenta crystal was mounted on a glass fiber in a random orientation on an Enraf-Nonius CAD-4 automatic diffractometer. The radiation used was Mo Kα which was monochromatized by a dense graphite crystal assumed for all purposes to be 50% imperfect. Final cell constants, as well as other information pertinent to data collection and refinement, are listed in Table I. The Laue symmetry was determined to be $P2/m$, and from the systematic absences noted, the space group was unambiguously shown to be $P2_1/c$. Intensities were measured by using the θ–2θ scan technique, with the scan rate depending on the net count obtained in rapid prescans of each reflection. Two standard reflections were monitored periodically during the course of the data collection, and these did not vary significantly. This provided a check of crystal stability and electronic reliability. In reducing the data, Lorentz and polarization factors were applied, as well as an empirical absorption correction based on azimuthal ψ scans of six reflections having χ near 90°.[10]

The unit cell has only two formula weights, and this implies that for the $P2_1/c$ space group the porphyrin unit must lie around an inversion center. The structure was solved by assuming the Ir atom to be at $^1/_2$, $^1/_2$, $^1/_2$. Unfortunately, this means that the Cl$^-$ and CO ligands must necessarily be 50:50 disordered and this disorder was included in the crystal structure solution. The position of Cl$^-$ was determined from interpretation of the Patterson map, based on a Ir–Cl distance of 2.40 Å. Additional solvent molecules of crystallization were found in the ratio of two benzonitrile molecules per porphyrin unit. The usual sequence of isotropic and anisotropic refinement was followed, after which all hydrogens were entered in ideally calculated positions. The hydrogen isotropic temperature factors were estimated on the basis of the thermal motion of the associated carbons. All non-hydrogen atoms except the disordered Cl and CO were refined anisotropically. After all shift/estimated standard deviation ratios were less than 0.5, convergence was reached; final values of $R = 2.3\%$ and $R_w = 2.5\%$ were obtained. No unusually high correlations were noted between any of the variables in the last cycle of least-squares refinement, and the final difference density map showed no peaks greater than 0.30 e/Å^3. All calculations were made by using Molecular Structure Corp.'s TEXRAY 230 modifications of the SDP-PLUS series of programs.

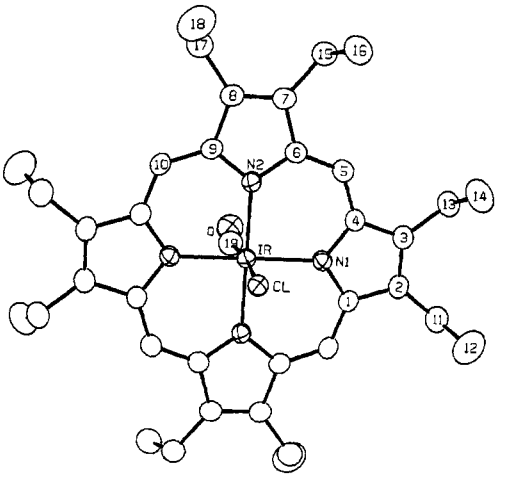

Figure 1. Molecular structure and numbering scheme of (OEP)Ir(CO)Cl.

Results and Discussion

Crystal Structure of (OEP)Ir(CO)Cl. The molecular structure and numbering scheme of (OEP)Ir(CO)Cl is represented in Figure 1, while Table II gives the final atomic positional parameters. The geometry about the iridium atom can be described as octahedral. The Ir atom is in the N_4 plane of the porphyrin macrocycle, as expected for a metalloporphyrin with an axial ligand above and below the porphyrin plane. However, due to the assignment of Ir at an inversion center, no deviation from the N_4 plane was observed.

The Ir–carbon bond distance is 1.95 Å, and the Ir–Cl bond distance is 2.29 Å. Both bond distances are typical for Ir–CO[11–13] and Ir–Cl[12] distances in non-porphyrin structures. The Ir–C–O angle is 167°, which is lower than the 176–177° range reported for Ir–C–O in non-porphyrin structures. The lower Ir–C–O angle observed in (OEP)-Ir(CO)Cl may reflect the 50/50 disorder observed between Cl and CO. The average Ir–N distance of 2.05 Å is the same as that observed for (OEP)Ir(C_8H_{13}).[8] Tables III and IV give select bond distances and angles, respectively. All of the bond distances and angles of the octaethylporphyrin macrocycle are within the expected ranges.[8,14–16]

(9) Lin, X.-Q.; Kadish, K. M. *Anal. Chem.* **1985**, *57*, 1498.
(10) Noth, A. C. T.; Phillips, D. C.; Mathews, F. S. *Acta Crystallogr., Sect. A: Cryst. Phys., Diffr., Theor. Gen. Crystallogr.* **1968**, *A24*, 351.
(11) Reis, A. H.; Hagley, V. S.; Peterson, S. W. *J. Am. Chem. Soc.* **1977**, *99*, 4184.
(12) La Placa, S. J.; Ibers, J. A. *Inorg. Chem.* **1966**, *5*, 405.
(13) Rasmussen, P. G.; Anderson, J. E.; Bailey, O. H.; Tamres, M.; Bayon, J. C. *J. Am. Chem. Soc.* **1985**, *107*, 279.
(14) Takenaka, A.; Syal, S. K.; Sasada, Y.; Omura, T.; Ogoshi, H.; Yoshida, Z. *Acta Crystallogr., Sect. B: Struct. Crystallogr. Cryst. Chem.* **1976**, *B32*, 62.
(15) Grigg, R. *Acta Crystallogr., Sect. B: Struct. Crystallogr. Cryst. Chem.* **1982**, *B38*, 2455.

Table II. Positional Parameters and Their Estimated Standard Deviations

atom	x	y	z
Ir	0.500	0.500	0.500
C1	0.6342 (3)	0.5552 (2)	0.5947 (1)
O	0.3294 (8)	0.4229 (5)	0.3753 (3)
N1	0.3491 (4)	0.6215 (3)	0.5022 (2)
N2	0.3516 (4)	0.4147 (3)	0.5552 (2)
N3	0.2029 (6)	0.8461 (4)	0.2776 (2)
C1	0.3672 (5)	0.7148 (3)	0.4729 (2)
C2	0.2323 (5)	0.7780 (3)	0.4840 (2)
C3	0.1333 (5)	0.7208 (3)	0.5200 (2)
C4	0.2056 (5)	0.6223 (3)	0.5309 (2)
C5	0.1430 (5)	0.5413 (4)	0.5650 (2)
C6	0.2088 (5)	0.4461 (3)	0.5772 (2)
C7	0.1381 (5)	0.3643 (3)	0.6126 (2)
C8	0.2372 (5)	0.2832 (3)	0.6113 (2)
C9	0.3710 (5)	0.3147 (3)	0.5749 (2)
C10	0.5021 (5)	0.2565 (3)	0.5615 (2)
C11	0.2090 (6)	0.8845 (4)	0.4595 (2)
C12	0.2653 (8)	0.9639 (4)	0.5056 (3)
C13	−0.0248 (5)	0.7502 (4)	0.5451 (2)
C14	−0.0164 (6)	0.7826 (5)	0.6179 (3)
C15	−0.0163 (5)	0.3725 (4)	0.6459 (2)
C16	−0.0011 (6)	0.4266 (4)	0.7126 (2)
C17	0.2130 (6)	0.1784 (4)	0.6396 (2)
C18	0.2569 (7)	0.1670 (5)	0.7109 (3)
C19	0.405 (1)	0.4481 (8)	0.4166 (5)
C20	0.3832 (5)	0.7104 (4)	0.2277 (2)
C21	0.4331 (6)	0.7224 (4)	0.1640 (3)
C22	0.5368 (7)	0.6521 (5)	0.1402 (3)
C23	0.5886 (7)	0.5728 (5)	0.1796 (3)
C24	0.5368 (7)	0.5618 (4)	0.2428 (3)
C25	0.4351 (6)	0.6301 (4)	0.2671 (2)
C26	0.2807 (6)	0.7851 (4)	0.2545 (3)
H5	0.0410	0.5517	0.5821
H10	0.5014	0.1885	0.5777
H11A	0.0934	0.8953	0.4496
H11B	0.2653	0.8918	0.4167
H12A	0.2446	1.0321	0.4847
H12B	0.2078	0.9578	0.5477
H12C	0.3798	0.9543	0.5147
H13A	−0.0677	0.8081	0.5168
H13B	−0.0970	0.6902	0.5399
H14A	−0.1231	0.8024	0.6319
H14B	0.0261	0.7260	0.6460
H14C	0.0554	0.8439	0.6229
H15A	−0.0911	0.4125	0.6157
H15B	−0.0590	0.3028	0.6527
H16A	−0.1069	0.4304	0.7321
H16B	0.0721	0.3874	0.7428
H16C	0.0401	0.4970	0.7058
H17A	0.0995	0.1600	0.6329
H17B	0.2776	0.1288	0.6137
H18A	0.2379	0.0952	0.7245
H18B	0.3712	0.1837	0.7175
H18C	0.1931	0.2149	0.7367
H21	0.3975	0.7783	0.1371
H22	0.5712	0.6603	0.0961
H23	0.6610	0.5240	0.1614
H24	0.5732	0.5062	0.2701
H25	0.3995	0.6225	0.3113

Table III. Selected Bond Distances (Å) of (OEP)Ir(CO)Cl

atom 1	atom 2	dist
Ir	Cl	2.292 (2)
Ir	N2	2.046 (2)
Ir	N1	2.046 (2)
Ir	C19	1.949 (7)

Electrochemistry of (P)Ir(CO)Cl. The electrochemistry of (P)Ir(CO)Cl was investigated in CH_2Cl_2, PhCN, and THF containing 0.1 M $TBAClO_4$. Each compound could undergo two oxidations and two reductions at low temperature or fast scan rate. Cyclic voltammograms showing the two oxidations and the first reduction of (OEP)Ir(CO)Cl in CH_2Cl_2 are given at −60 and 5 °C in parts a and b, respectively, of Figure 2. A rotating disk voltammogram of (OEP)Ir(CO)Cl in CH_2Cl_2 is shown in Figure 2c. The voltammograms of (OEP)Ir(CO)Cl show two reversible oxidations at $E_{1/2}$ = 1.05 and 1.53 V vs. SCE.[17] There is an irreversible room-temperature reduction at E_p = −1.48 V, but this reaction is reversible at −60 °C and occurs at $E_{1/2}$ = −1.59 V. Under these conditions a second irreversible reduction occurs at ~−1.8 V. This reduction was not investigated in detail. In the same solvent/supporting electrolyte system (TPP)Ir(CO)Cl is reversibly oxidized at $E_{1/2}$ = 1.22 V and reversibly reduced at $E_{1/2}$ = −1.16 V. There is also a second irreversible oxidation at ~−1.7 V.

Table IV. Selected Bond Angles (deg) of (OEP)Ir(CO)Cl

atom 1	atom 2	atom 3	angle
Cl	Ir	N1	91.72 (7)
Cl	Ir	N2	88.70
Cl	Ir	C19	174.5 (3)
N1	Ir	N2	89.48 (7)
N1	Ir	C19	87.1 (2)
N2	Ir	C19	91.7 (2)
Ir	C19	O	167.8 (7)

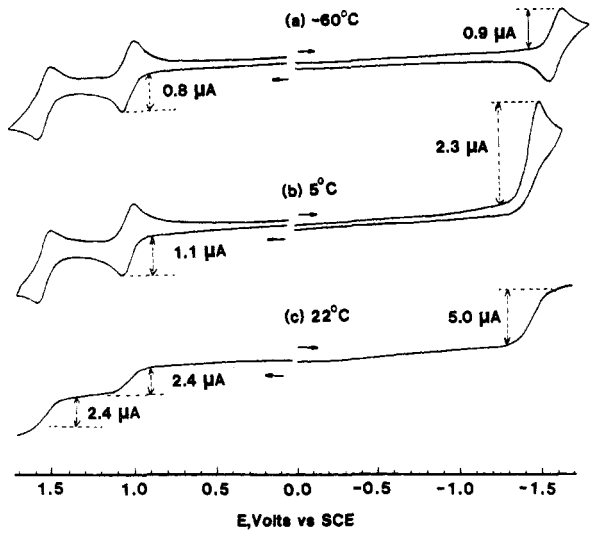

Figure 2. Cyclic voltammograms (200 mV/s) of (OEP)Ir(CO)Cl in CH_2Cl_2, 0.1 M $TBAClO_4$ at (a) −60 °C, (b) 5 °C, and (c) rotating disk voltammogram (10 mV/s, 800 rpm).

The irreversible first electroreduction of (OEP)Ir(CO)Cl was investigated by variable scan cyclic voltammetry, and the peak potential was found to shift by −33 mV per 10-fold increase in scan rate. This shift of E_p is shown in Figure 3a and agrees with theoretical shifts for an irreversible chemical reaction following a diffusion-controlled one-electron transfer.[18] The difference between the peak potential and half-peak potential was 60 ± 5 mV at all scan rates, further indicating a reversible one-electron transfer in the initial electroreduction.

Rotating disk experiments show that the peak current ratio between the first reduction and the first oxidation at low rotation rate is about equal to 2.0, suggesting a two-electron reduction. This was confirmed by bulk con-

(16) Cullen, D. L.; Meyer, E. F.; Smith, K. M. *Inorg. Chem.* **1977**, *16*, 1179.

(17) Reference 7 erroneously assigned the oxidation of (OEP)Ir(CO)Cl at 1.18 V vs. SCE (1.05 V vs. SCE in our study) as a *two-electron reduction* of Ir^{III} to give an Ir^{I} species. However, the rotating disk experiment in Figure 1a clearly indicates that this electrode reaction is an *oxidation* which involves only *one electron*. The spectroelectrochemical data presented in this paper also agree with such a formulation.

(18) Nicholson, R. S.; Shain, I. *Anal. Chem.* **1964**, *36*, 706.

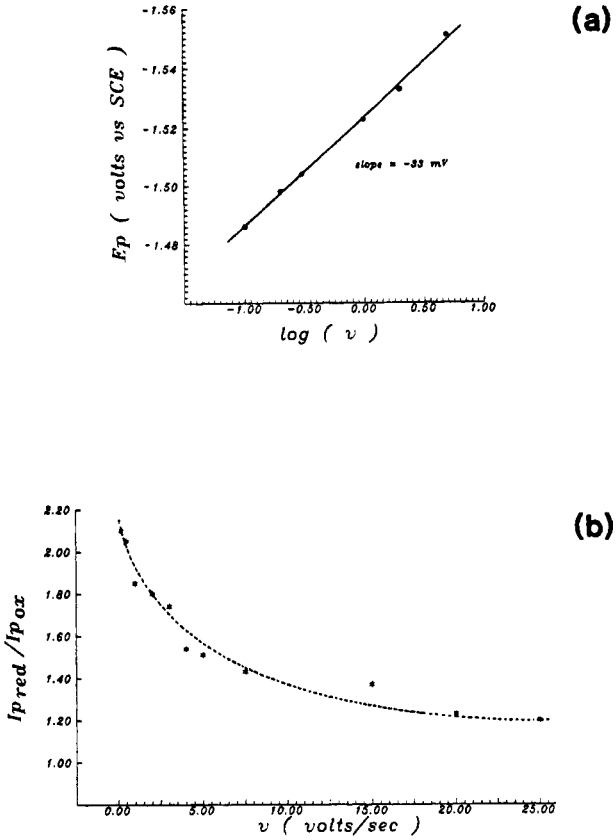

Figure 3. (a) Plot of the peak potential (E_p) for the reduction of (OEP)Ir(CO)Cl in CH_2Cl_2 as a function of log (v). (b) Plot of the ratio of the first reduction and first oxidation currents for (OEP)Ir(CO)Cl as a function of the scan rate at +5 °C in CH_2Cl_2. Data were taken from a voltammogram such as the one shown in Figure 2b.

trolled potential electrolysis. The first oxidation of (OEP)Ir(CO)Cl gave a value of one electron per mole while the first reduction required two electrons for completion.

Similar results are obtained by cyclic voltammetry. At low potential scan rates, the ratio of reduction to oxidation peak currents is 2.05 (see Figure 2b). This ratio is scan rate dependent and approaches unity as the scan rate is increased. This is illustrated in Figure 3b for the oxidation and reduction of (OEP)Ir(CO)Cl at 5 °C. At low temperature (−60 °C), the first reduction is reversible, and under these conditions the ratio of reduction to oxidation peak currents is unity (see Figure 2a).

The chemical reaction following electroreduction of (OEP)Ir(CO)Cl generates $[(OEP)Ir]^-$ as shown in eq 2.

$$(OEP)Ir(CO)Cl + 2e \rightarrow [(OEP)Ir]^- + CO + Cl^- \quad (2)$$

Cyclic voltammograms for the reduction of (OEP)Ir(CO)Cl were identical in CH_2Cl_2 independent of the supporting electrolyte (0.1 M $TBAClO_4$ or 0.1 M TBACl) and gas above the solution (1 atm of CO or N_2). This lack of CO or Cl^- dependence on the voltammogram rules out the dependence on an equilibrium involving CO or Cl^-.

The peak current for reduction of (OEP)Ir(CO)Cl is approximately twice as large as peak current for the first oxidation that involves a reversible one-electron transfer. In addition, no reverse reoxidation peak is observed after the addition of two electrons (see Figure 2b). This behavior is expected for an electrochemical ECEC-type mechanism (a mechanism where two electron transfers are separated by a chemical reaction and where the second electron transfer is followed by another chemical reaction). The data are also consistent with an overall reaction in which both the first and second electron transfers involve

Table V. Half-Wave Potentials (V vs. SCE) of (P)Ir(CO)Cl in CH_2Cl_2, THF, and PhCN Containing 0.1 M $TBAClO_4$

product	solv	temp, °C	2nd ox.	1st ox.	1st red.
(TPP)Ir(CO)Cl	CH_2Cl_2	22		1.25	−1.15
	PhCN	22		1.25	−1.15
	THF	22			−1.17
(OEP)Ir(CO)Cl	CH_2Cl_2	22	1.45	1.05	−1.48[a]
	CH_2Cl_2	−78	1.44	1.07	−1.59
	PhCN	22	1.46	1.06	−1.49[a]
	THF	22			−1.49[a]
	THF	−78			−1.61

[a] E_{pc} at 0.1 V/s.

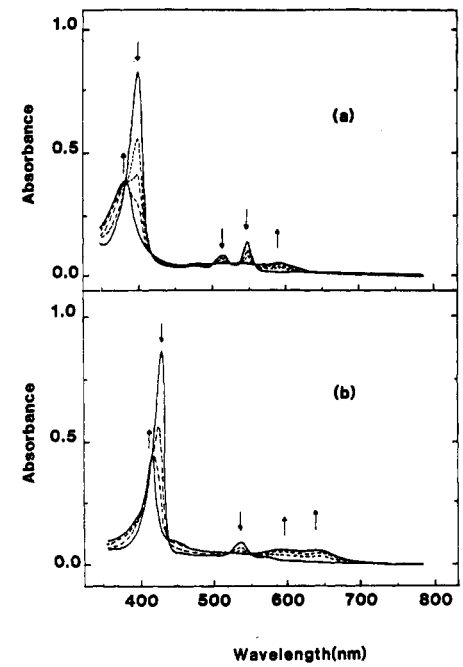

Figure 4. UV–visible spectral changes observed during the oxidation of (a) (OEP)Ir(CO)Cl and (b) (TPP)Ir(CO)Cl in PhCN, 0.1 M $TBAClO_4$.

a one-electron reduction and where the two chemical reactions are irreversible.[19]

(TPP)Ir(CO)Cl differs from (OEP)Ir(CO)Cl in that it exhibits a reversible one-electron room temperature reduction, at scan rates as low as 0.05 V/s. However, at longer time scales such as are needed for thin-layer electrochemistry or bulk electrolysis, a total of two electrons are consumed in the reduction. Thus the same type of reduction mechanism probably occurs as for the OEP derivative, but in the case of the TPP complex the chemical reaction following the first one-electron addition is too slow to affect the cyclic voltammogram. A similar electrochemistry was observed for (TPP)Ir(CO)Cl in benzonitrile and in THF, and half-wave and peak potentials for oxidation and reduction of the complex in these solvents are summarized in Table V.

Spectral Monitoring of Oxidized (P)Ir(CO)Cl. Figure 4a shows the spectral changes that occur during the first oxidation of (OEP)Ir(CO)Cl in benzonitrile. The original product has a Soret band at 404 nm and two Q bands at 519 and 549 nm. As oxidation goes to completion, the Soret band shifts to 385 nm and decreases in intensity while a broad absorption band appears in the range between 500 and 650 nm. A set of isobestic points is observed at 388, 424, 527, 537, and 557 nm, and the original spectrum

(19) (a) Nicholson, R. S.; Shain, I. *Anal. Chem.* **1965**, *37*, 178. (b) Savéant, J.-M. *Electrochim. Acta* **1967**, *12*, 753.

Table VI. Maximum Absorbance Wavelengths (λ_{max}) and Corresponding Molar Absorptivities (ϵ) for Oxidized and Reduced (OEP)Ir(CO)Cl and (TPP)Ir(CO)Cl

compd	solv	λ_{max}, nm ($10^{-3}\epsilon$)		
(OEP)Ir(CO)Cl	CH_2Cl_2	403 (170)	516 (11.4)	548 (28.1)
	THF	403 (178)	516 (11.3)	548 (28.2)
	PhCN	404 (174)	519 (12.0)	549 (29.3)
$[(OEP)Ir(CO)Cl]^+$	CH_2Cl_2	384 (74)	550 (sh)	595 (10.9)
	PhCN	385 (75)	548 (sh)	596 (11.2)
$[(OEP)Ir]^-$	PhCN	383 (77)	503 (23.4)	
	THF	382 (70)	503 (22.8)	
(TPP)Ir(CO)Cl	CH_2Cl_2	420 (395)	531 (36.8)	556 (sh)
	THF	420 (390)	531 (39.0)	567 (sh)
	PhCN	421 (405)	530 (39.3)	566 (sh)
$[(TPP)Ir(CO)Cl]^+$	CH_2Cl_2	411 (187)	587 (23.3)	638 (24.1)
	PhCN	412 (190)	585 (22.4)	635 (23.7)
$[(TPP)Ir]^-$	THF	398 (217)	495 (17.9)	
	PhCN	397 (215)	495 (18.4)	

could be regenerated by back reduction at a potential more negative than 0.95 V. The final oxidized spectrum is typical of a porphyrin π cation radical,[20] and this assignment was confirmed by ESR spectroscopy. Singly oxidized (OEP)Ir(CO)Cl exhibits an ESR signal centered at $g = 2.00$ with a peak-to-peak separation of 5–10 G, a value typical of porphyrin π cation radicals.[20]

Similar types of spectral changes were observed during oxidation of (TPP)Ir(CO)Cl. This is shown in Figure 4b while Table VI summarizes the wavelengths for the maximum absorbances and molar activities of neutral and singly oxidized (TPP)Ir(CO)Cl.

Spectral Monitoring of Reduced (P)Ir(CO)Cl. Figure 5a shows changes that occur in the electronic absorption spectra during the two-electron reduction of (OEP)Ir(CO)Cl in THF at room temperature. The neutral (OEP)Ir(CO)Cl has absorptions at 403, 516, and 548 nm. Upon the initial reduction this spectrum is transformed to a spectrum that exhibits a Soret band at 382 nm and a Q band at 503 nm. Isosbestic points are observed at 385, 421, and 513 nm and indicate that any generated reduced intermediates react extremely rapidly compared to the experimental time scale. The final spectrum of the reduced product has bands at 382 and 503 nm and has earlier been characterized as the spectrum of $[(OEP)Ir]^-$.[2,7,8] The totally reduced (OEP)Ir(CO)Cl is ESR silent and does not exhibit a CO stretch in the 2500–1800 cm^{-1} region of the infrared spectrum. This indicates the loss of CO upon reduction.

At room temperature, the overall electrode reaction of (OEP)Ir(CO)Cl is given by eq 2 and the spectrally detected species on the thin-layer time scale are (OEP)Ir(CO)Cl and $[(OEP)Ir]^-$. However, completely different spectral changes are observed when the reduction of (OEP)Ir(CO)Cl is performed at low temperature (see Figure 5b for reduction at −70 °C). No isosbestic points are seen, indicating the presence of more than two species in solution. The final product has absorption bands at 441, 600, and 760 nm that are typical of a porphyrin π anion radical. The reduced solution exhibited a weak ESR signal at 120 K that was centered at $g = 2.00$ and had a peak-to-peak separation of 10 G. Reoxidation of the reduced solution at −1.0 V showed that 0.3 electron was consumed in the reoxidation at −70 °C and that only 25% of the original material could be recovered as calculated by UV–visible spectroscopy. All of these data are consistent with a decrease in the rate of the chemical reaction or reactions following the first electron transfer and the spectral monitoring of at least three species: the initial (OEP)Ir(CO)Cl, the final $[(OEP)Ir]^-$, and an ESR-active intermediate.

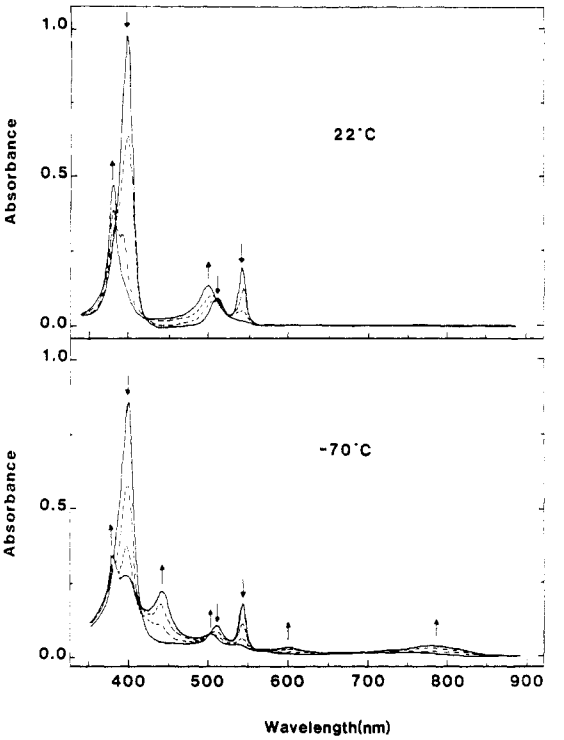

Figure 5. UV–visible spectral changes observed during the reduction of (OEP)Ir(CO)Cl in THF, 0.3 M $TBAClO_4$ at (a) 22 °C and (b) −70 °C.

The low-temperature spectral results are consistent with the low-temperature cyclic voltammetry data which show a one-electron reversible reduction at −70 °C. The appearance of porphyrin π anion radical absorption bands indicates that the first electron transfer occurs at the porphyrin π ring system to form the intermediate $[(OEP)Ir^{III}(CO)Cl]^-$ species. The obtaining of $[(OEP)Ir]^-$ as the final reduction product implies an intramolecular electron transfer between the porphyrin π ring system and the Ir(III) metal of $[(OEP)Ir(CO)Cl]^-$. A similar sequence of steps was reported to occur during reduction of $(OEP)Ir(C_8H_{13})$, which also yields $[(OEP)Ir]^-$ as a final product.[8]

Acknowledgment. The support of the National Science Foundation (Grant No. CHE-8515411) is gratefully acknowledged.

Registry No. (OEP)Ir(CO)Cl, 68324-58-3; (TPP)Ir(CO)Cl, 109432-33-9; $[(OEP)Ir(CO)Cl]^+$, 109432-34-0; $[(OEP)Ir^I]^-$, 109432-35-1; $[(TPP)Ir(CO)Cl]^+$, 109432-36-2; $[(TPP)Ir^I]$, 109432-37-3; $[(OEP)Ir(CO)Cl]^-$, 109432-38-4; (OEP)Ir(CO)Cl·PhCN, 109432-39-5.

Supplementary Material Available: The cell packing diagram and full tables of bond angles, bond distances, and general temperature factors for the structural determination of (OEP)Ir(CO)Cl (4 pages). Ordering information is given on any current masthead page.

(20) Kadish, K. M. *Prog. Inorg. Chem.* **1986**, *34*, 435.